A New Method for Predicting the Solar Heat Gain of Complex Fenestration Systems

J.H. Klems **J.L. Warner**

ABSTRACT

A new method of predicting the solar heat gain through complex fenestration systems involving nonspecular layers such as shades or blinds has been examined in a project jointly sponsored by ASHRAE and DOE. In this method, a scanning radiometer is used to measure the bidirectional radiative transmittance and reflectance of each layer of a fenestration system. The properties of systems containing these layers are then built up computationally from the measured layer properties using a transmission/multiple-reflection calculation. The calculation produces the total directional-hemispherical transmittance of the fenestration system and the layer-by-layer absorptances. These properties are, in turn, combined with layer-specific measurements of the inward-flowing fractions of absorbed solar energy to produce the overall solar heat gain coefficient.

This method has been used to determine the solar heat gain coefficient of a double-glazed window with an interior white shade. The resulting solar heat gain coefficient was compared to a direct measurement of the same system using the MoWiTT (Mobile Window Thermal Test) Facility for measuring window energy performance, and the two results agreed. This represents the first in a series of planned validations and applications of the new method.

INTRODUCTION

Solar heat gain has become an increasingly important and complex aspect of the continuing effort to make windows more energy efficient. On one hand, the usual strategy of reducing summer cooling loads by limiting solar heat gain has been complicated by the increasing recognition that the use of daylight with proper lighting controls can produce substantial energy savings in commercial buildings, a strategy that argues for high visible transmittance. Building energy simulation studies (Choi et al. 1984) show that window management yields both peak and annual energy savings and, in fact, assume that some form of shading for glare control is necessary for any successful daylight utilization. On the other hand, recent measurements (Klems 1989, 1982) show that solar heat gain is an important determinant of the winter energy performance of windows. While sophisticated (i.e., building simulation model-based) calculations of window performance would include the effect of winter solar gain, all too frequently discussions of winter performance have been based on simplified calculations that considered only changes in U-value. The effect of solar gain on winter performance is particularly important in residences, where a large percentage of windows have some form of shading or privacy device. Thus, it is not possible to calculate window performance either in winter or summer without considering solar gain, and it is necessary to address the issue of solar gain through windows with nonspecular shading devices (such as shades, blinds, etc.), which we term "complex fenestration systems."

The traditional method of determining complex fenestration system performance is by measurement in a solar calorimeter, (Parmelee et al. 1948, 1953; Ozisik and Schutrum 1959; Yellott 1965; Pennington et al. 1964) but a systematic characterization by this method poses some daunting problems. Shades, blinds, and drapes vary widely in reflectance, transmittance, and color. Moreover, the optical properties of venetian blinds vary with slat tilt angle. All of them may be combined with glazings of various numbers of panes, pane thicknesses, and tints and coatings. To construct a solar heat gain rating system analogous to the NFRC U-value method (NFRC 1991), it would be necessary for a manufacturer to determine the performance of a product line (possibly containing many products that differ only in color and surface pattern) in combination with every possible glazing system (as well as every adjustment configuration for systems such as venetian blinds). To do this by calorimeter, measurement for each distinct combination would require a prohibitive amount of testing. On the other hand, to construct an analytical model of the type that has sometimes appeared in the literature (Farber et al. 1963) for each specific type of shading device would be a large research effort, for which many of the essential heat transfer data are not currently available.

Therefore, it would be useful to devise a method of calculating solar heat gain that is intermediate between the extremes of calorimetric measurement and first-principles calculation, enabling one to calculate the solar heat gain through complex fenestration systems from a smaller and more easily obtained set of measurements. We have been developing and validating such a method in a research project sponsored jointly by ASHRAE and the U.S. Department of Energy. In this paper we summarize this work and present preliminary data on the method's feasibility.

Joseph H. Clems is a staff scientist and **Jeff H. Warner** is a senior research associate in the Building Technologies Program, Energy and Environment Division, Lawrence Berkeley Laboratory, Berkeley, CA.

A NEW METHOD FOR CALCULATING SOLAR HEAT GAIN

We begin by examining the usual expression for the solar heat gain coefficient, F, of a fenestration system,

$$F = \tau + N_I \alpha \ , \qquad (1)$$

where τ and α are the transmittance and absorptance, respectively, and N_I is the inward-flowing fraction of the absorbed solar energy. If we recognize (1) that this quantity inherently depends on the solar incident angle, θ; (2) that for a device not cylindrically symmetrical (such as a blind, which has a preferred direction, the slat orientation), it may also depend on the angle, ϕ, between a characteristic direction and the plane of incidence; and (3) that the fenestration consists of M layers denoted by i, then we can generalize Equation 1 to make it valid for any fenestration system:

$$F(\theta,\phi) = T_{fH}(\theta,\phi) + \sum_{i=1}^{M} N_i A_{fi}\ (\theta,\phi) \ , \qquad (2)$$

where T_{fH} denotes the front directional-hemispherical transmittance of the *system*, and N_i, A_{fi} denote the inward-flowing fraction and front absorptance, respectively, of the ith layer. The layer inward-fraction, N_i represents the fraction of the energy absorbed in the ith layer that ultimately flows into the building space and is the analog of N_I in Equation 1. We next observe that T_{fH} and A_{fi} are purely optical quantities, depending on such properties as wavelength and reflectance but not on temperature, while N_i is a calorimetric quantity that may depend on the geometry of the fenestration system, as well as on temperatures and other heat transfer variables, but not on the short-wavelength properties of the system, such as color or reflectance.

This observation suggests a simplification. T_{fH} could be determined by an optical measurement using a large integrating sphere, a much simpler and more rapid measurement than a calorimetric measurement. A measurement of N_i would necessarily be a calorimetric measurement, but it could be made once for a particular geometry of fenestration system and subsequently applied to all systems of that geometry, regardless of their optical properties. If there were also an optical method of measuring A_{fi}, then a single set of N_i ($i = 1, \ldots, M$) could be combined with rapid optical measurements to characterize a whole set of systems of differing optical properties. For example, a shade manufacturer wishing to characterize a product line of 25 different colors and patterns in combination with N possible glazing systems would need to make $25 \times N \times N$ optical transmittance and absorptance measurements on the systems rather than the same number of more lengthy calorimetric measurements.

We have carried the simplification one step further by considering how the directional-hemispherical transmittance T_{fH} might also be built up from layer measurements. If we consider, for example, a two-layer system as shown in Figure 1, we can consider the progress of a ray of radiation incident on the first layer as due to the action of linear transformations on the ray, with $\Im_1(x_1)$ transforming the ray incident on layer 1 at point x_1 into a transmitted intermediate ray at the same point, $\Lambda_{21}(x_2,x_1)$, propagating the ray to point x_2 in layer 2, and $\Im_2(x_2)$ transforming the intermediate ray into the final outgoing ray. In this language of linear transformations, a product of transformations is, in fact, an integral. For example, if we neglect interreflections between the two layers, the transmission of the system in Figure 1 would be

$$\Im_2 \cdot \Lambda_{21} \cdot \Im_1 = \int \Im_2(x_2)\Lambda_{21}(x_2,x_1)\Im_1(x_1)\,dx_1 \ , \qquad (3)$$

where the points x_1 and x_2 determine the angles of the intermediate ray. The integration over x_1 means that for a nonspecular layer 1, any point in the layer can produce an outgoing ray that reaches a given point x_2. Equation 3 is meant to be physically illustrative rather than mathematically precise; for instance, the transformation $\Im_1(x_1)$ also depends on the incident angle and on x_2, dependences that have been suppressed for simplicity. Similarly, we have left out multiple interreflections (which would be very cumbersome to include using the notation of Equation 3), although these are an essential part of the method and will be included below.

In order to make this description mathematically tractable and useful, two simplifications are desirable. First, we are interested in the total amount of transmitted radiation and its angular distribution but not in its detailed spatial distribution across the fenestration system (i.e., in the plane of the fenestration layers); we also do not attempt to treat edge effects. While shading devices such as blinds and

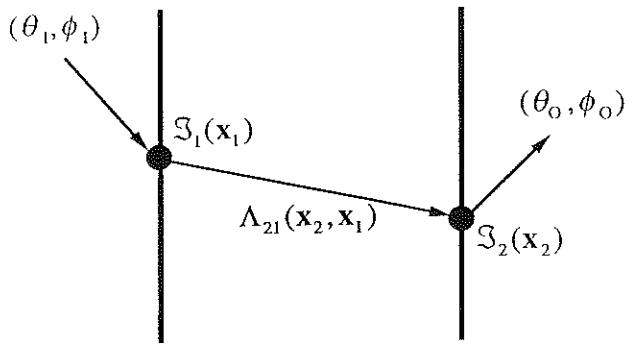

Figure 1 *Schematic diagram of the transmittance of a ray through a two-layer fenestration system, seen as a series of linear transformations on the ray. Multiple reflections of the ray have been omitted from the diagram for simplicity.*

drapes are spatially nonuniform, we may average over spatial regions that are large compared to the dimension characteristic of their nonuniformity (e.g., weave spacing or slat width) and treat the resulting average as a spatially uniform layer. This will still give us the quantity of interest, the total transmittance, and we can then drop the overall spatial dependence in Equation 3. This means that we can shift from the point representation of Equation 3 to a representation depending only on angles. Second, by considering all measurements to be made on a finite grid of angles, all of the integrals in the problem may be approximated by the multiplication of finite-dimensional matrices. With these simplifications, the total front transmittance, including interreflections, of the two-layer system in Figure 1 may be written as

$$T_f = T_2 \cdot (1 - \Lambda_{21} \cdot R_1 \cdot \Lambda_{12} \cdot R_2)^{-1} \cdot \Lambda_{21} \cdot T_1 , \qquad (4)$$

where each of the quantities in the equation is a finite-dimensional matrix. The elements of the matrix T_1 are the biconical (front) transmittances of layer 1, and those of R_1 are the biconical (back) reflectances. The matrix Λ_{21} (note the ordering of the indices) is a diagonal matrix representing the propagation of radiation from layer 1 to layer 2: essentially, it converts outgoing radiance (at a particular angle) to incoming irradiance (at the same angle). The superscript "-1" indicates the inverse matrix. We note that the inverse matrix indicated in the equation (the quantity in parentheses) represents the summation of an infinite series of multiple reflections between layers 1 and 2. The layer transmittance and reflectance matrices, for example, T_1 and R_1, are constructed by dividing the incom-incoming and outgoing angle hemispheres into a finite number of pieces, each characterized by its central direction angles (θ,ϕ). These pieces are then numbered in a predetermined way and ordered to form a (column) vector of incoming angles $(\theta,\phi)_j$ and a (row) vector of outgoing angles $(\theta,\phi)_i$. An element T_{ij} of the layer transmittance matrix then gives the biconical transmittance from the incoming angular element $(\theta,\phi)_j$ into the outgoing angular element $(\theta,\phi)_i$. The diagonal propagation matrix matches up incoming and outgoing directions, and, for consecutive layers, the normal rules of matrix multiplication ensure that the product of transmittances will contain a sum over all the intermediate rays at various angles. Each layer may thus have arbitrary optical properties, subject only to the assumptions listed above: the properties may be treated as spatially averaged quantities, and angular variations are adequately represented by the finite angular grid chosen. Most fenestration systems of practical interest should satisfy these assumptions. We note in this treatment that a specular layer appears as a diagonal matrix. We also note that the use of matrix multiplication and the chosen identification of incoming and outgoing radiation with rows and columns enforces a particular ordering of the elements in Equation 4: progression of radiation through the system corresponds to moving from right to left in Equation 4.

We can summarize the essential results of the method without further burdening the reader with either the derivation or the mathematical details. Some of these, including the general outline of the method, have been presented previously (Papamichael et al. 1988), and the complete derivation will be a part of the final report to ASHRAE on the project. For any fenestration system consisting of layers, the biconical solar-optical transmittance of the system over a grid of incident and outgoing directions can be determined from the biconical transmittance and reflectance matrices of the individual layers by an expression analogous to Equation 4. The dimensions of the matrices necessary depend on the symmetry of the individual layers and on the angular accuracy necessary: specular layers (e.g., glass) are represented by diagonal matrices containing the directional transmittances/reflectances. The directional-hemispherical transmittance and the layer-by-layer absorptances of the system are similarly readily calculated. The determination of F as a function of incident direction for a particular device in a given fenestration system then requires

- measurement of the bidirectional (or biconical) transmittances and reflectances of the nonspecular device,
- knowledge of the solar-optical properties of the other layers of the system (e.g., glass properties),
- calorimetric measurement of the layer's inward-flowing fractions N_i for the particular geometric and thermal system configuration under consideration,
- calculation of the system's directional-hemispherical transmittances and layer-by-layer absorptances, and
- calculation of the solar heat gain coefficient, $F(\theta,\phi)$, using Equation 2.

To return to the example of the shade manufacturer with a 25-product line, using this method it would be necessary to make 25 bidirectional transmittance and reflectance measurements and possibly to share with other manufacturers the cost of a series of generic calorimetric measurements of fenestration system inward-flowing fractions. Presumably the properties of the other layers would be available from their manufacturers (e.g., glass properties). The manufacturer would then need to make only 25×2 solar-optical measurements (or 25×4 if the front- and back-transmittances and reflectances of the product are different) instead of $25 \times N \times N$. Although the solar-optical measurements required are complex, they may still be performed more rapidly (and presumably, more economically) than calorimetric measurements, and the possibility of spreading the cost of the necessary calorimetry and eliminating the combinatorial problem (i.e., that a separate measurement is needed for each shade/glazing combination) gives this method potential advantages in both speed and economy.

MEASUREMENT OF BICONICAL OPTICAL PROPERTIES

It was first necessary to develop an apparatus capable of measuring the biconical transmittance and reflectance of a sample of dimensions large enough to provide a reasonable average over periodic device features such as blind slats. Ideally, one would have liked to use a sample on the order of a full window size, 1 m^2. Unfortunately, this would have made the apparatus prohibitively large and expensive. We settled for a design sample size of 10 in. × 10 in. and ended with a usable sample size of 7.5 in. × 7.5 in.

We constructed a large, automated scanning radiometer, shown in Figures 2 and 3. In this apparatus, a calibrated detector measures the outgoing radiation at a large

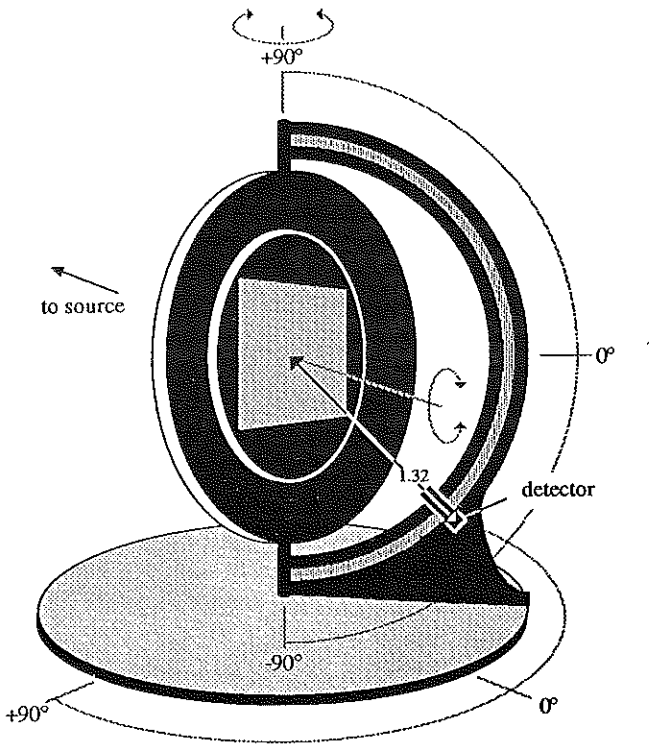

Figure 2 *Schematic diagram of the scanning radiometer. The apparatus consists of a fixed light source and a sample mounted on a plane that rotates about a fixed vertical axis relative to the source to produce an incident angle, θ. The sample also rotates about an axis perpendicular to this plane to produce an incident azimuth angle, ϕ. The detector is mounted on a semicircular arm that rotates through the outgoing azimuth angle, γ, about a vertical axis through the center of the sample. The detector moves up and down over this semicircular arm to vary the probe altitude angle, β, producing an angular coverage over the entire outgoing hemisphere relative to the sample.*

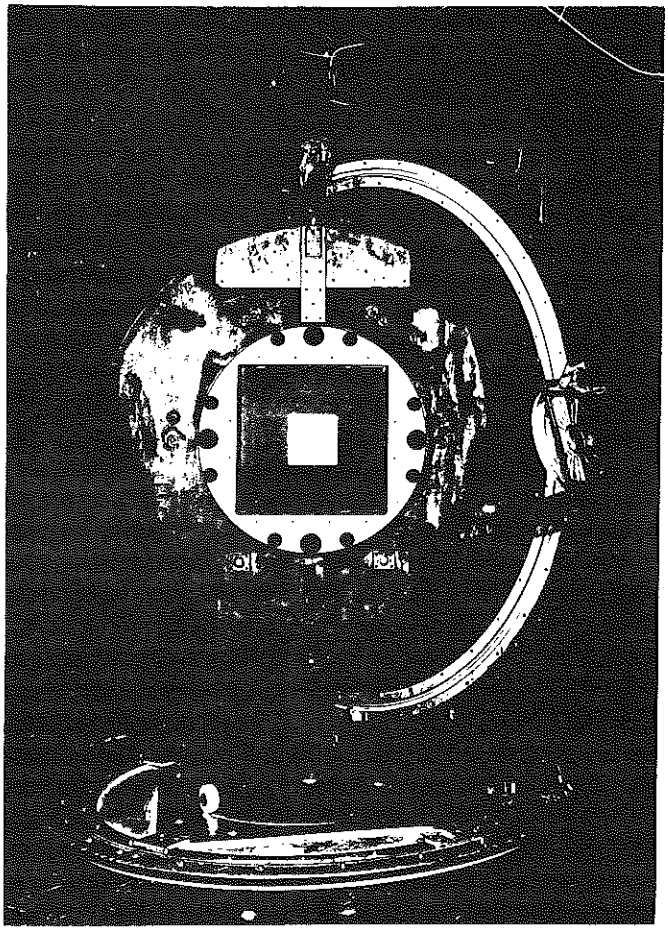

Figure 3 *Photograph of the scanning radiometer. The detector arm is shown in the hemisphere toward the light source, measuring bidirectional reflectance.*

number of angular positions distributed over either the front or rear outgoing hemisphere, and this measurement is repeated for all combinations of incident angles that it is necessary to sample, depending on the inherent symmetry of the layer under test. Biconical transmittance and reflectance are determined from these measurements and the measured incident irradiance. Both radiometric (350-2200 nm) and photometric data are recorded simultaneously.

The detector optical system is shown in Figure 4. Radiation within a narrow angular cone around the detector axis is focused on the entrance port of an integrating sphere that contains the detector elements. The collection system is characterized by high demagnification and high angular dispersion. Light collection is insensitive to position within the sample plane until the cone of angular acceptance originating at a point in the sample plane begins to clip the edge of the collection mirror. It is this effect that limits the size of the usable sample.

The apparatus was first calibrated with open-sample-port transmission measurements and later using a 7.5 $in.^2$ lambertian reflector of known (approximately 98%) hemi-

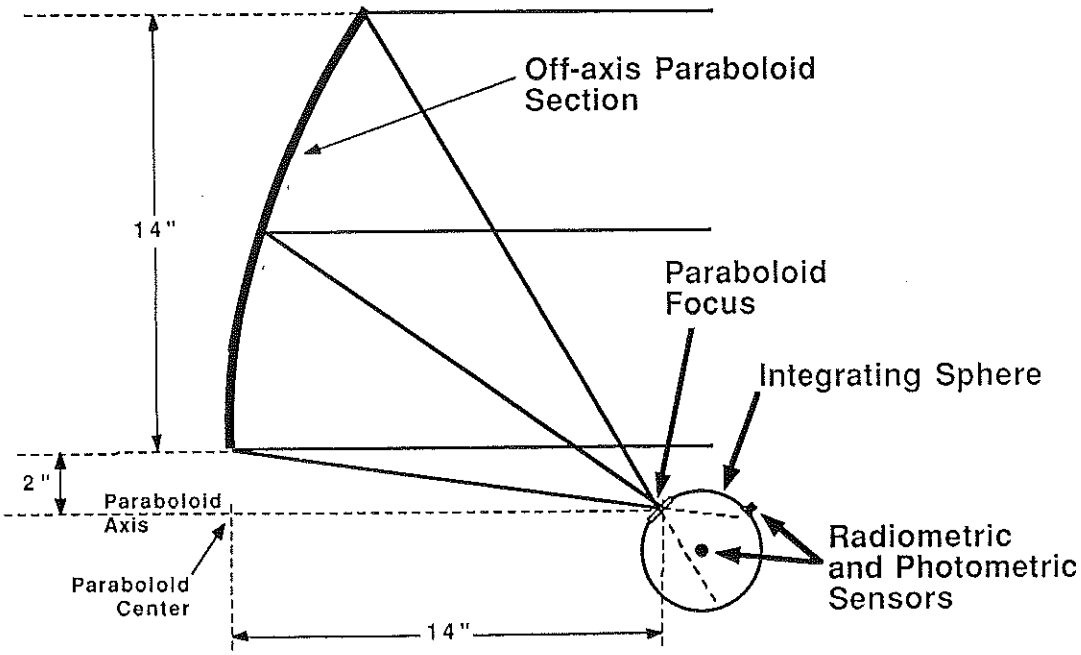

Figure 4 *Scanning radiometer detector optical collection system. Light parallel to the axis of the detection system is collected by an off-axis parabolic mirror and focused onto the entrance port of an integrating sphere containing both radiometric and photometric sensors. Radiometric and photometric data are recorded simultaneously. This scheme provides wavelength-independent collection of radiation from a large sample area, combined with a sharp angular selectivity. Wavelength sensitivity is determined by the reflectance characteristics of the integrating sphere interior coating and is good from 350 to 2200 nm.*

spherical reflectance, uniform with wavelength over the 350-2200 nm region. The two calibration procedures agreed to within 1% for moderate angles, and the calibrated-reflector measurements were used to determine the apparatus efficiency at large angles. As a first test of the new solar heat gain calculation method, the characteristics of a diffusing white shade were measured and are shown in Figure 5.

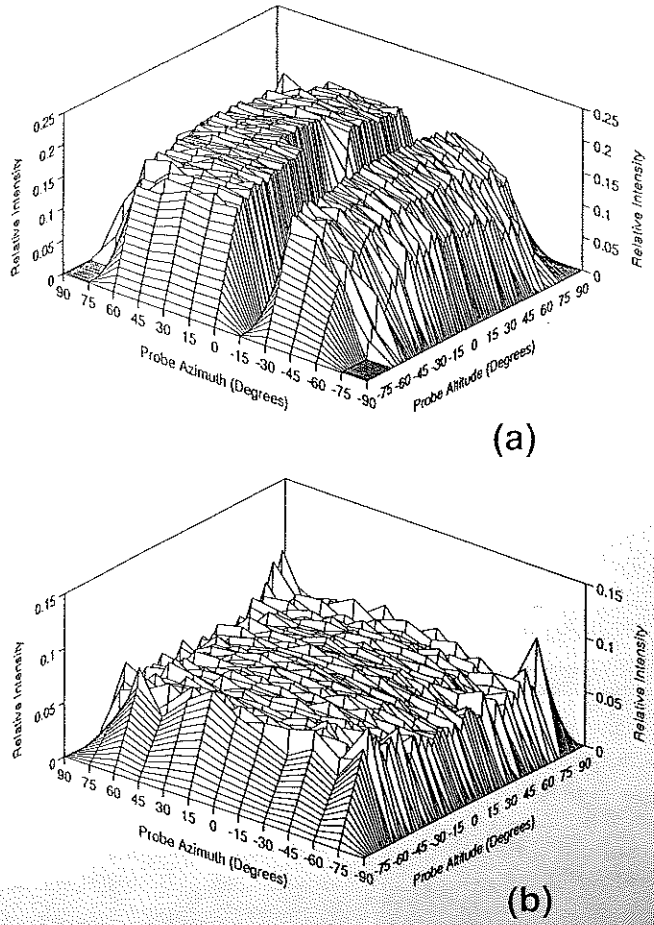

Figure 5 *Scanning radiometer measurements of (a) reflectance and (b) transmittance of a translucent white shade. The deep valley in the reflectance distribution is an experimental artifact caused by obstruction of the light beam by the detector and its supporting arm (see Figure 2). The detector geometry prevents measurements beyond outgoing altitudes of $\pm 70.5°$, and data outside these limits are disregarded. In addition, the apparent reflectance dips and transmittance peaks at extreme detector azimuths are due to still unresolved experimental difficulties with surround reflectance, noise, and collection geometry and are also disregarded.*

MEASUREMENT OF INWARD-FLOWING FRACTION

The inward-flowing fractions N_i of the absorbed solar energy are the only inherently calorimetric quantities in the determination of the solar heat gain coefficient. In principle, they depend on the temperatures of the layers and their surroundings, air temperatures, and air motion. In previous discussions in the literature, they have variously been treated as constants (Yellott 1966) or evaluated theoretically using an idealized heat transfer model (Farber et al. 1963). The physical processes that produce the N_i are both understandable and complex. Solar energy absorbed in a particular layer of a fenestration system will divide into inward and outward heat flow in proportion to the ease with which it can flow in the two directions under the prevailing conditions. But this depends on the temperature of the layer in question, of the adjacent layers, and of the adjacent air; in addition, the pattern and velocity of adjacent airflow may have an effect, and all of these may depend on the level of solar irradiation. For the outer fenestration layer, wind and exterior air and radiative temperatures would be expected to be important.

For all of these reasons, the N_i were measured under realistic indoor and outdoor conditions. Evaluating the extent to which they vary with external weather conditions was an important part of defining the method. Clearly, if the N_i showed a high degree of variability, providing a representative set of values for solar heat gain calculations would be a much more difficult task than if the variability were low.

We performed these inward-flowing fraction measurements in Reno, NV, using the Mobile Window Thermal Test (MoWiTT) facility for measuring window energy performance (Klems et al. 1982). This facility consists of two side-by-side room-sized guarded calorimeters. To measure the value of N_i for a layer in a particular fenestration system, identical fenestration systems were mounted in the two calorimeters, with provision made to electrically heat the selected layer in one of the fenestrations. Electrical heat applied to that layer would simulate a small increase in solar absorptance, and if a fraction N_i of the applied power, P, flowed inward, then the net heat flowing through the fenestration would increase by an amount N_iP. Since the calorimeter accurately measures the net heat flow and P is also known, varying P and measuring the resulting change in net heat flow gave a direct measurement of N_i. In this measurement, the companion calorimeter with the unheated layer acted as a control.

Initial investigations using this method for a between-pane venetian blind established that the N_i are relatively insensitive to temperature variations. We first needed to establish that the temperature rise of the blind due to the application of the electrical power was not large enough to perturb seriously the behavior of N_i. We found that application of an amount of power that gave a measurable value for N_iP resulted in a change in blind temperature of a few degrees Celsius, while the night-to-day swing in blind temperature under summer conditions was much larger, on the order of 40°C. There was no significant difference between day- and nighttime measurements of N_i. We concluded from this that (1) the electrical heating method did not significantly affect the physical situation and (2) the N_i had no significant temperature dependence, at least for the fenestration configuration examined. In fact, in subsequent measurements, we have been unable to find evidence for temperature dependence in any system, a somewhat surprising phenomenon. The analysis of inward-flowing fraction data is not yet complete; consequently, this is a tentative conclusion. Similarly, the N_i do not appear to depend significantly on wind or other weather conditions, with the possible exception of the exterior layer. Such a dependence would certainly be expected to be significant for exterior glazing layers or exterior blinds. We have not yet investigated this issue because, as will be seen, the inward-flowing fraction for exterior glass layers is quite small.

In practice it proved impossible to set up identical situations in the two calorimeter chambers for many shading devices, most notably Venetian blinds. The combination of irregularities in slat shape and variability in tilt angle made the "identical" systems demonstrably different. Therefore, we ultimately used an analytical method that compares each shading device to itself. The tests were performed by first running for several days with the layer heating power turned off, next setting the power to a fixed value for several days, and finally running again for several days with the power off. The data taken were fit with the following equation:

$$W(t) = D \cdot [T_o(t) - T_I(t)] + B \cdot I_s(t) + N_i \cdot P(t), \quad (5)$$

where D, B, and N_i are constants determined by fitting the data, and the other quantities in the equation are measured as functions of time in the MoWiTT. An example of this fitting procedure is shown in Figure 6.

VALIDATION OF THE METHOD

The MoWiTT facility also provides a way of directly checking the results of the solar heat gain factor determination method. In Equation 5 (above) the quantity $I_s(t)$ is the vertical-surface solar intensity incident on the window. It is directly measured using a pyranometer placed on the vertical surface adjacent to the two calorimeters. The constant B determined in the fit is, therefore, simply $<F> \cdot A_G$, where A_G is the glazed area of the window and $<F>$ is the effective value of the solar heat gain coefficient, which is a solar-intensity-weighted average over the set of solar incident angles occurring during the test period. The constant D is obviously also related to the U-value, but in these summer tests, a number of experimental factors make its value a poor basis for determining nighttime U-value.

A direct measurement of $<F>$ can be compared to a calculation of $<F>$ from scanning radiometer and inward-

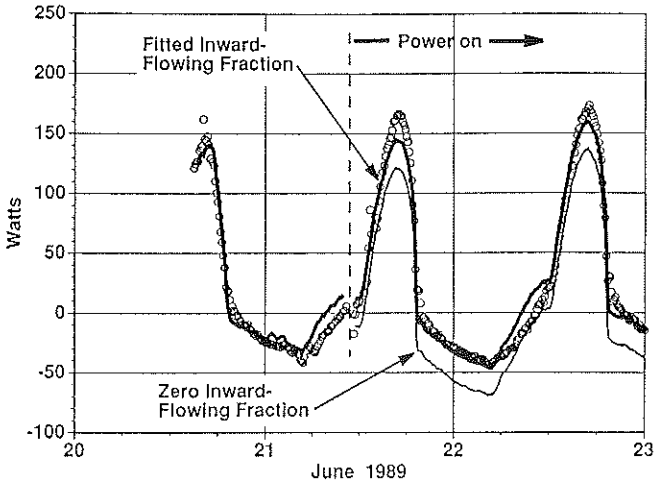

Figure 6 *Determination of inward-flowing fraction for an interior shade. The MoWiTT measurement of the apparent net heat flow through the window (open circles) is plotted with the calculated curve for the fitted value of* N_i *(heavy curve) given by Equation 5. Comparison with the same calculation assuming* N_i = *O (light curve) gives a measure of the significance of the determination. The two curves coincide before the blind was electrically heated. The fact that the model of Equation 5 does not accurately fit the measured points in the morning or near the solar intensity peak is probably related to the assumption of a constant value of* F.

flowing fraction measurements. We have made this comparison for the first device measured with the scanning radiometer, the translucent white shade of Figure 5. This shade was mounted on the interior of a wood-framed window with clear double glazing and measured in a west-facing orientation. The measured net energy flow through the window was fit to the equation

$$W(t) = D \cdot [T_o(t-\delta) - T_I(t-\delta)] + \langle F \rangle \cdot A_G \cdot I_S(t-\delta) \quad (6)$$

to determine the constants D, $<F>$, and δ. (The constant δ accounts for the finite thermal response time of the calorimeter.) In Figure 7, the data are shown together with the fitted curve. The resulting value of $<F>$ was 0.36 $\pm$ 0.04. The plot of $I_s(t)$ as a function of the solar incident angle in Figure 8 shows that the incident angle was in the range 20° to 60° when the solar intensity was greatest. The intensity-weighted mean solar incident angle calculated from this plot was $<\theta>$ = 46.95°.

RESULTS

The scanning radiometer measurement distributions in Figure 5 are characteristic of a diffusing material at all but the extreme outgoing angles, where there are decreases in the reflectance distribution and apparent peaks in the transmittance. However, these are experimental artifacts caused by surround reflectance, noise, and problems with the collection geometry at extreme angles. These problems will be resolved as we refine our experimental procedure. At present, the evidence of Figure 5 is that the shade is perfectly diffusing; if we accept this conclusion, then we can conclude from the measurement that its transmittance is 0.21 and its reflectance is 0.62.

The inward-flowing fraction measurements for an interior shade with double glazing are not yet completed. Measurements have been completed for an interior venetian blind with single and double glazing and an interior shade with single glazing, results for which are shown in Table 1. It is clear from the table that the value of N_i for the innermost (shading) layer depends on the geometry of the layer. For a downward-tilted blind, adding another glazing layer raises the value of N_i significantly; an interior shade appears to have a value of N_i greater than that for a downward-tilted blind but slightly less than that for a closed blind. From this, we can conclude only that an interior shade with double glazing should have $0.68 < N_i < 1$, and we estimated a value of 0.84 $\pm$ 0.16. For the glass layer inward-flowing fractions, we used the values for an interior venetian blind with double glazing, incorporating the probable errors in this choice into the uncertainty estimates.

We used the matrix method described above to calculate the directional-hemispherical transmittances of the system and the directional layer absorptances on a 15° grid of incident angles. Combining these with the inward-flowing fractions produced the solar heat gain coefficient as a function of incident angle, shown in Figure 9. The directional-hemispherical transmittance and layer absorptances were also linearly interpolated to obtain the values at $<\theta>$ = 46.95°. These were combined with the estimated inward-flowing fractions, as indicated in Table 2, to produce a value of the solar heat gain coefficient, $F(<\theta>)$ = 0.33 $\pm$ 0.04.

DISCUSSION

The value of the effective solar heat gain coefficient computed using the new method, $F(<\theta>)$ = 0.33 $\pm$ 0.04, is in excellent agreement with the value $<F>$ = 0.36 $\pm$ 0.04 measured with the MoWiTT. This first treatment of a relatively well-known system augurs well for the overall success of the project, which will repeat this comparison for a number of different shading devices and fenestration systems. This comparison implicitly assumes the equality of the intensity-weighted angular average $<F>$ and the value of F at the intensity-weighted average angle $<\theta>$. This assumption should be valid, since F is a slowly varying function of θ over the angles of appreciable solar intensity, as can be verified by comparing Figures 8 and 9.

The dominant source of error in the scanning radiometer determination of F for the white shade is the uncertainty

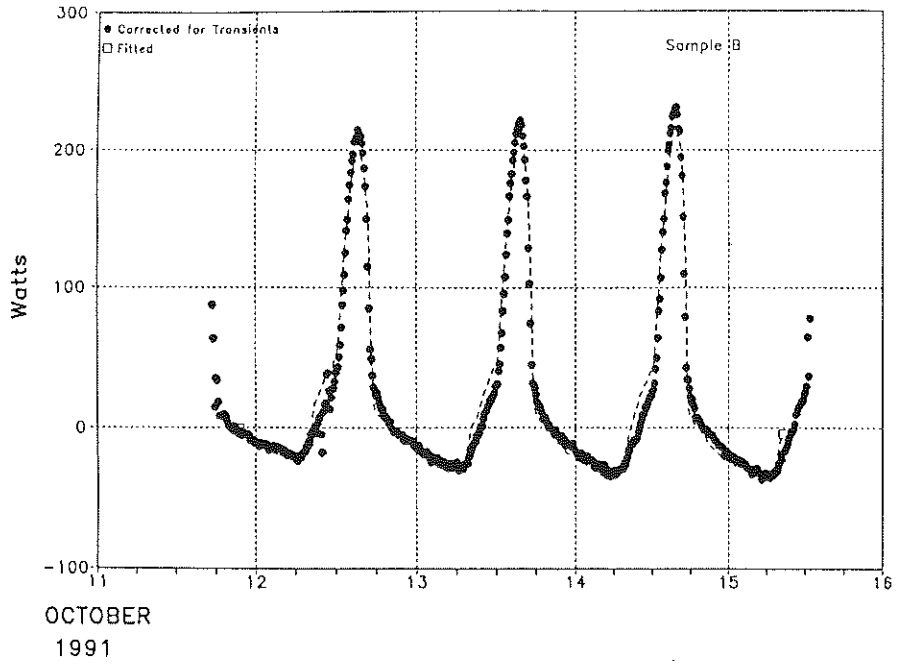

Figure 7 *Calorimetric determination of the solar heat gain coefficient for double glazing with an interior white shade. The MoWiTT measurements of the net heat flow through the window (points) is compared to the model of Equation 6 (dashed curve) using the values of the fitted parameters given in the text.*

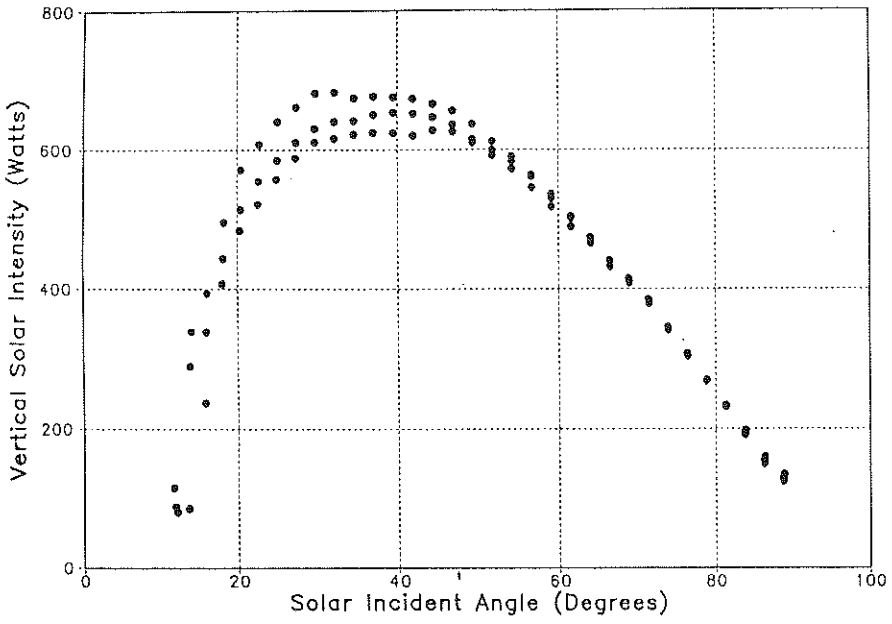

Figure 8 *Vertical solar intensity incident on the window as a function of solar incident angle for double glazing with an interior white shade.*

in the estimate of inward-flowing fractions. When these estimates are replaced by measurements, the overall experimental uncertainty should improve, making the comparison between scanning radiometer determination and MoWiTT measurement a more stringent test.

The transmittance and reflectance of the measured shade are very similar to the properties of "translucent light roller shades" in Tables 27.26 and 27.28 of the *ASHRAE Handbook* (ASHRAE 1989), for which the listed shading coefficient implies a solar heat gain coefficient of 0.35 at a 30° incident angle. If we repeat the above calculation assuming the transmittance and reflectance used in the ASHRAE table (0.25 and 0.60, respectively), we obtain a value of $F=0.36$ at 30°, indicating that our method is

TABLE 1
Measurements of Layer Inward-Flowing Fractions of Several Fenestration Systems

System	Adjust-ment	Measured N_i		
		Shading Layer	Inner Glass	Outer Glass
Single/ Interior Venetian Blind	45° up	0.34 ± 0.03		-0.02 ± 0.04
	Closed	0.68 ± 0.01		0.12 ± 0.01
	30° down	0.57 ± 0.02		0.21 ± 0.02
Single/ Interior Shade		0.64 ± 0.01		0.15 ± 0.01
Double/ Interior Venetian Blind	45° down	0.68 ± 0.03	0.50 ± 0.03	0.19 ± 0.01

TABLE 2
Derivation of Solar Heat Gain Coefficient

Quantity	Value	N_i	Contribution to Solar Heat Gain Coefficient
System Directional-Hemispherical Transmittance	0.17 ± 0.02		0.17 ± 0.02
Shade Absorptance	0.13 ± 0.02	0.84 ± 0.16	0.11 ± 0.03
Inner Glass Absorptance	0.048 ± 0.005	0.5 ± 0.1	0.024 ± 0.005
Outer Glass Absorptance	0.112 ± 0.005	0.2 ± 0.1	0.02 ± 0.01
Total			**0.33 ± 0.04**

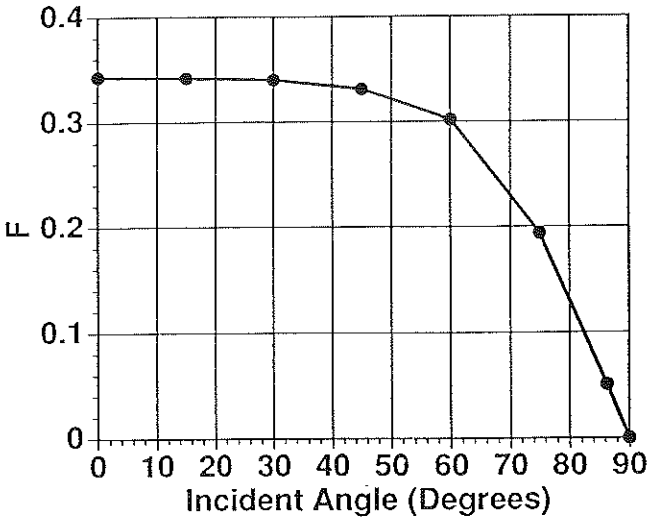

Figure 9 *Solar heat gain coefficient as a function of solar incident angle determined using the proposed method.*

consistent with that previously used by ASHRAE, at least in this instance.

CONCLUSION

We have described a new method of determining the solar heat gain coefficient for complex fenestration systems by calculation from measured layer biconical optical properties and generic system calorimetric properties. The latter could be compiled in a data base and applied to a large number of systems.

A method and apparatus for measuring the biconical solar-optical properties of fenestration layers have been developed, as has a method of measuring layer inward-flowing fractions.

The determination has been applied to a double-glazed window with an interior shade, and the resulting calculated solar heat gain coefficient was consistent with a direct calorimetric measurement on the same system. For a very similar fenestration system listed in the *ASHRAE Handbook*,

the calculation method gives a result in reasonable agreement with the ASHRAE value.

These preliminary results indicate that the method is viable, and we plan to extend it to a variety of complex fenestration systems.

ACKNOWLEDGMENTS

The authors are grateful for the efforts of Mark Spitzglas, who participated in the early stages of scanning radiometer design and construction; of Konstantinos Papamichael, who made important contributions to the conceptual and early software development of the project; and of Ramalingam Muthukumar, who assisted in the later development of the analysis software. The efforts of Dennis DiBartolomeo, Mary Hinman, Jonathan Slack, and Mehrangiz Yazdanian were vital to the completion and automation of the scanning radiometer. Special thanks are due to Guy Kelley and the MoWiTT operational team, Steve Lambert and Michael Streczyn, whose patient and continuous efforts over several years resulted in the inward-flowing fraction measurements.

This research was jointly supported by ASHRAE, as Research Project 548-RP under Agreement No. BG 87-127 with the U.S. Department of Energy, and by the Assistant Secretary for Conservation and Renewable Energy, Office of Building Technologies, Building Systems and Materials Division of the U.S. Department of Energy under Contract No. DE-AC03-76SF00098.

REFERENCES

ASHRAE. 1989. *1989 ASHRAE Handbook—Fundamentals.* Atlanta: American Society of Heating, Refrigerating and Air-Conditioning Engineers.

Choi, U.S., R. Johnson, and S. Selkowitz. 1984. The impact of daylighting on peak electrical demand. *Energy and Buildings* 6:387.

Farber, E.A., W.A. Smith, C.W. Pennington, and J.C. Reed. 1963. Theoretical analysis of solar heat gain through insulating glass with inside shading. *ASHRAE Transactions* 69:392.

Klems, J.H. 1989. U-values, solar heat gain and thermal performance: Recent studies using the MoWiTT. *ASHRAE Transactions* 95(1):609.

Klems, J.H. 1982. Net energy performance measurements on two low-E windows. Report No. LBL-32128, Lawrence Berkeley Laboratory.

Klems, J.H., S. Selkowitz, and S. Horowitz. 1982. A mobile facility for measuring net energy performance of windows and skylights. *Proceedings of the CIB W67 Third International Symposium on Energy Conservation in the Built Environment*, Vol. 3, 3.1. Dublin, Ireland: An Foras Forbartha.

NFRC (National Fenestration Rating Council). 1991. *NFRC 100-91: Procedure for determining fenestration product thermal properties (Currently limited to U-values).* Silver Spring, MD.

Ozisik, N., and L.F. Schutrum. 1959. Heat flow through glass with roller shades. *ASHRAE Transactions* 65:697.

Papamichael, K., J. Klems, and S. Selkowitz. 1988. Determination and application of bidirectional solar-optical properties of fenestration systems. *Proceedings of the 13th National Passive Solar Conference*, Massachusetts Institute of Technology, Cambridge.

Parmelee, G.V., W.W. Aubele, and D.J. Vild. 1953. The shading of sunlit glass. *ASHVE Transactions* 59:221.

Parmelee, G.V., W.W. Aubele, and G. Huebscher. 1948. Measurements of solar heat transmission through flat glass. *ASHVE Transactions* 54:158.

Pennington, C.W., W.A. Smith, E.A. Farber, and J.C. Reed. 1964. Experimental analysis of solar heat gain through insulating glass with indoor shading. *ASHRAE Transactions* 70:54.

Yellott, J.I. 1965. Drapery fabrics and their effectiveness in solar heat control. *ASHRAE Transactions* 71:260.

Yellott, J.I. 1966. Shading coefficients and sun-control capability of single glazing. *ASHRAE Transactions* 72:72.